World Academy of Science, Engineering and Technology
International Journal of Mechanical and Mechatronics Engineering
Vol:15, No:9, 2021

Empirical Analysis of Velocity Behavior for Collaborative Robots in Transient Contact Cases

C. Schneider, M. M. Seizmeir, T. Suchanek, M. Hutter-Mironovová, M. Bdiwi, M. Putz

Open Science Index, Mechanical and Mechatronics Engineering Vol:15, No:9, 2021 publications.waset.org/10012307.pdf

***Abstract*—**In this paper, a suitable measurement setup is presented to conduct force and pressure measurements for transient contact cases at the example of lathe machine tending. Empirical measurements were executed on a selected collaborative robot's behavior regarding allowable operating speeds under consideration of sensor- and workpiece-specific factors. Comparisons between the theoretic calculations proposed in ISO/TS 15066 and the practical measurement results reveal a basis for future research. With the created database, preliminary risk assessment and economic assessment procedures of collaborative machine tending cells can be facilitated.

***Keywords*—**Biomechanical thresholds, collaborative robots, force and pressure measurements, machine tending, transient contact.

I. Introduction

IN the last decade, machine tending became an established application for collaborative robots (cobots). Small and medium-sized enterprises (SME's) with high-mix-low-volume production programs increasingly benefit from the high flexibility of robotic machine loading and unloading. The main benefit in human-robot-collaboration lies in the fast and convenient system adaptation to new requirements and fenceless operation. Despite the evident benefits, particular attention must be paid to the extensive risk assessment, especially regarding the force and pressure measurements defined in ISO/TS 15066. Thereby, the compliance to body-region-specific biomechanical threshold values of the robot's movements relative to the velocity must be verified, delivering the actual cycle times. Since a prototypical cell is required to conduct these tests, the project must already be well-advanced for validating the targeted operating times. However, for economic considerations, a preliminary database of realistic velocities and, therefore, cycle times would be beneficial to approximate the return on investment (ROI) of an automation project upfront. This is also relevant for alternative investment considerations, such as industrial robots or linear systems. Currently, end-users and system integrators have only the ISO/ TS 15066 as a guideline, which provides equations to calculate the allowed collaborative speed for the transient contact case. Alternatively, the standard proposes the option to execute respective force and pressure measurements. Modeling the system parameters that influence the velocity result and demonstrated risk assessment studies are lacking and do not meet the expectation of new cobot users.

This study aims to derive more insights on maximum allowable collaborative speeds (MACS) of cobots. Two typical risk cases with different collision angles of rotary workpieces were evaluated in detail, considering the influence of different sensor sensitivity settings and operating speeds on the force and pressure distribution. The results enable the planner to estimate the maximum allowed collaborative speed based on practical empirical data. Comparisons to the equations, as provided by the standards body, reveal research potentials for the future.

For the conduction of this study, a selected collaborative robot model has been used. Other cobots are welcomed to replicate this test setup and adapt the proposed measurement process and research method to contribute to this empirical database. In the future, exemplary velocity values for selected robots can serve as assistance to facilitate the planning and risk assessment process.

In this paper, we contribute to fundamental research in terms of influencing factors on the allowed collaborative speed in transient contact cases with a strong emphasis on biomechanical threshold values and respective forces and pressures.

II. Theory

References [1]-[5] give a general overview of safety aspects and concepts. Contact cases between human and robot are subdivided into quasi-static and transient ones. While the first type occurs in clamping situations in which continuously increasing weight is partially compensated by elastic deformation, the collision object maneuvers in the resultant direction from the impact in the second category. To avoid injuries of the operator, biomechanical threshold values for various body parts were defined based on human subject research. Empirical studies derived body-part-specific pain entrance levels that were transferred to ISO/TS 15066 [6]. In [7], several studies are presented with the purpose to refine and expand these values. To conduct a risk assessment for collaborative work cells, the whole system consisting of robot, gripper, and workpiece is critically assessed regarding potential contact cases. Since standards demand rounded edges of collaborative robot and gripper's outer contours, the critical system is usually the workpiece. Besides the physical robot system, the working environment and programmed robot paths must be included. The identified worst-case scenarios must be measured using either a prototypic or the actual commissioned cell. Therefore, designated measurement devices from different manufacturers are available, which enable the safety engineer to determine the occurring forces and pressures of a selected

C. Schneider is with Yaskawa Europe GmbH, Allershausen, Germany (e-mail: christopher.schneider@yaskawa.eu.com).

Open Science Index, Mechanical and Mechatronics Engineering Vol:15, No:9, 2021 publications.waset.org/10012307.pdf

contact situation. An integrated load cell measures the collision forces and delivers the time-dependent force applied to a respective software that generates a force graph over time. For pressure measurements, pressure indicating films in different resolutions are placed on top of the device. During the collision event, small air bubbles burst and discolor the film relative to the intensity. A scanner with respective software digitizes and visualizes the results. Besides the actual device, damping materials (K1) and a spring (K2) are used that simulate the single body parts by combination.

Since the current risk assessment procedure requires measurement of a specific situation, upfront determination of compliant velocities is not feasible. Adaptive safety systems that can adjust to dynamic environments (i.e., workpiece change), as presented in [8], would require a thorough understanding of influencing factors and the robot system behavior. In the following, different scientific approaches to analyze quasi-static and transient contact cases are summarized.

In [9], a three-dimensional map is presented that illustrates the collision forces relative to the robot's working space. Based on empirical measurements with the cobots UR10e and KUKA LBR Iiwa with the last robot joint, the influence of robot pose, distance, and velocity have been investigated. Reference [10] analyzed crash tests with different industrial robots considering the robot mass, velocity, and singularity forces during clamping. In [11], the power flux density is introduced as a factor by incorporating transferred energy and area, as well as contact duration. Furthermore, various influencing factors have been tested on the proposed rapid contact model. To reduce collision forces of the robot tool and the attached workpiece, a robotic airbag has been developed in [12] that has been evaluated regarding its effectiveness in empirical crash test dummy tests. Reference [13] introduces a multi-phase collision event procedure, which enables collision characterization and classification based on the force's direction and intensity as well as occurrence, severity, and duration. Models to calculate quasi-static forces were developed in [14], [15]. Virtual force sensors and simulations were presented in [16], [17].

III. Materials and Methods

A. Risk Assessment and Experimental Setup

Within a preliminary risk assessment for lathe machine tending applications, a transient contact case has been derived from the movement sequence illustrated in Fig. 1. During this operation, the robot moves from the machine's door (transparent) to the material position (opaque). If the worker is operating the machine or restacking workpieces, a collision with the hand can be anticipated. Therefore, the biomechanical threshold values of the back of the hand (non-dominant side, ND) are used for the further procedure. In the illustration, a double gripper can be seen, which is dominantly used in machine tending. For simplification reasons, this paper deals with single grippers. For comprehensive results, future research can analyze the influence of the gripper installation angle.

For this empirical study, a Yaskawa HC10DT IP67 collaborative robot with the software version YAS4.12.01A(EN/DE)-00 was used, which is installed on a robot pedestal. A metal base plate, where both the pedestal and a rigid frame were mounted upon, served as a solid structure. On top of the rigid frame, an adapter plate has been attached on which a guide rail was installed. Force and pressure were measured using the PILZ collision measurement set PRMS for collaborative robots following the specifications of ISO/TS 15066.

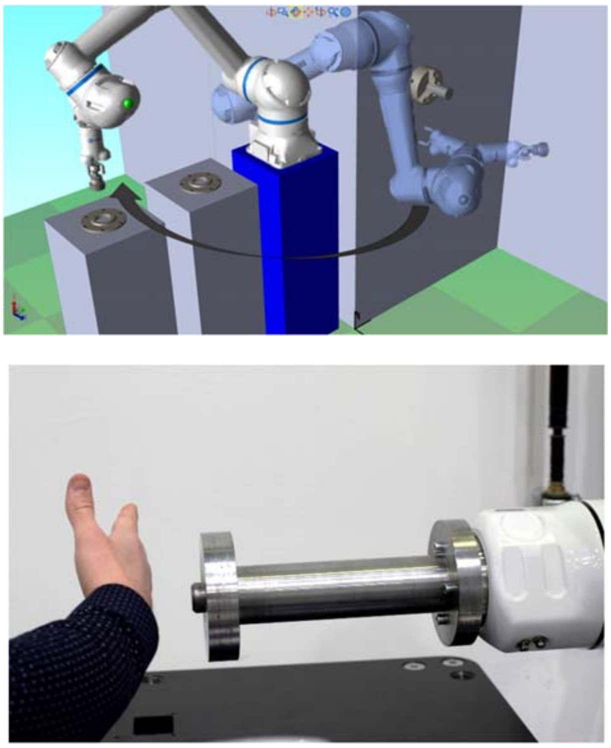

Fig. 1 Transient Contact Case

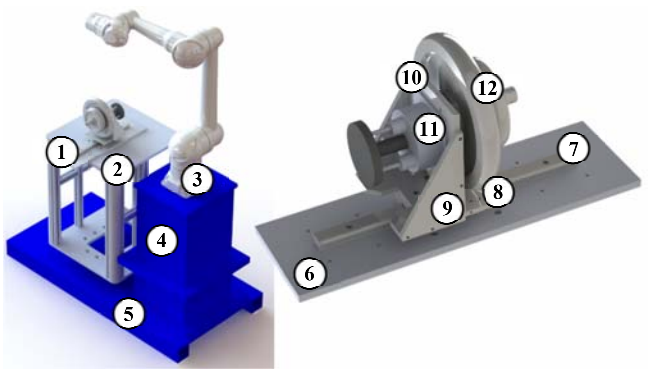

Fig. 2 Experimental Setup: 1 – Measurement Setup, 2 – Rigid Frame, 3 – Robot, 4 – Robot Pedestal, 5 – Base, 6 – Adapter plate, 7 – Guide rail, 8 – Rail carrier, 9 – Holding construction, 10 – Adapter plate for measurement device and locating bolt, 11 – Measurement device, 12 – Weight plates

B. Considered Influencing Factors

To understand the most critical influences on the measurement results, a list of potential factors with a criteria catalog for rotary workpieces has been developed in prior research [18]. This information builds the basis for measurement planning and execution. Figure 3 gives an overview of influencing factors, classified by the 5M's machine, method, material, (hu)man, and measurement. On this general basis, those factors have been specified with respective characteristics, which are summarized in Table I.

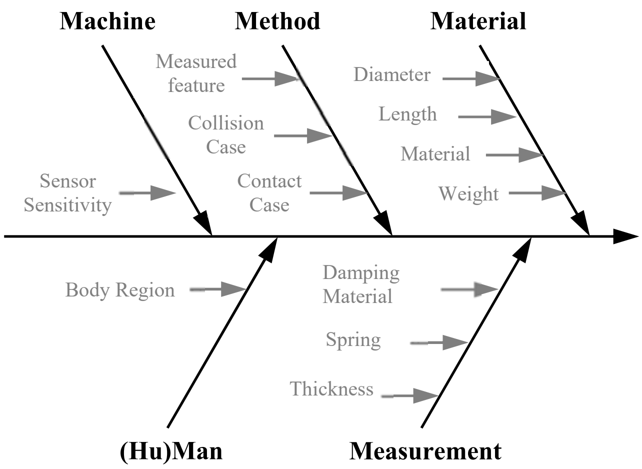

Fig. 3 Influencing Factors on the Collaborative Operating Speed

TABLE I
INFLUENCING FACTORS ON THE COLLABORATIVE OPERATING SPEED

5 M's	Criteria	Characteristics
Machine	Force Limit	140 N, 130 N, 100 N, 50 N
Machine	Software Version	YAS4.12.01A(EN/DE)-00
Machine	Measured Feature	Individual
Method	Collision Case	Transient
Method	Contact Case	Frontal, Lateral
(Hu)man	Allowed Pressure/ Force	P: 380 N/cm^2/ F: 280 N
Measurement	Damping Material K1	Shore A 70
Measurement	Spring K2	75 N/mm
Measurement	Thickness	7 mm
Material	Diameter	20 mm
Material	Length	230 mm
Material	Material	Steel
Material	Weight	6.041 kg

C. Experimental Design

In order to emulate the body regions' specific physical characteristics, technical drawings of a suitable measurement device were provided by the Fraunhofer Institute IFF, resulting from their latest research. It is designed for adjustment to the considered body regions' mass as defined in ISO/TS 15066 by adding appropriate weight plates if needed. In case of the hand region (m = 0.6 kg) this is not required, since the whole setup already weighs 3.8 kg, which can be considered as reality mismatching. We note that a setup design at 0.6 kg is not realistic due to the own weight of the measurement device and required stability to ensure replicable results. In future research, a conversion factor must be determined to deduce more realistic measurement results. According to [6] and [18], a spring with k = 75 N/mm, black silicone damping material with shore A 70 hardness, and a thickness of 7 mm must be used for the measurement device to match the back of the hand ND.

In the PRMS manual, three force measurements per series are recommended to counterbalance the device's inaccuracy. However, for this research, 10 measurement runs have been executed to provide scientific and statistically valid results. By excluding the maximum and minimum values (outliers), the eight remaining values were averaged for comparison to the defined biomechanical threshold values. Humidity and room temperature for the tests were measured at 60% and 21 °C on average, meeting the pressure-sensitive foils' limiting conditions of 35-80% humidity and a temperature range from 17 °C to 38 °C. To guarantee optimal foil development, a waiting time between pressure measurement and registry of at least 30 minutes has been adhered to.

To simulate a realistic collision with a workpiece, a steel shaft has been designed for simplification that matches the length and mass characteristics (d = 110 mm, l = 230 mm, m = 6.041 kg) of an industrial gripper with a small chuck part. For the collision itself, two different realistic cases have been derived from the beforementioned motion sequence: 1) plane contact with a round surface and 2) edge contact. Prior measurement studies on the diameter-dependent pressure impact from 110 mm to 20 mm show that 20 mm are critical. Therefore, the workpiece's surface has been turned to 20 mm in diameter to match these characteristics. In the second case, the robot was tilted by 45° while maintaining the same collision position. To determine the MACS, velocities are iteratively adjusted with a predefined scaling until one value exceeds the thresholds. The last compliant speed is the MACS. For the plane contact, a granularity of 1 mm/s is used since force is the dominant metric. However, for the edge contact, the scaling has been increased to 10 mm/s to reduce the measurement effort of scanning the single pressure-sensitive foils. For valid measurements of both cases, the distance between the initial position and the final position must be sufficiently high to ensure that the robot achieves the programmed operating speed. Also, the final position must be located at a fair distance behind the collision point to prevent the robot from decelerating before the impact. Tool data were configured, and torque sensors were calibrated regularly to ensure consistent measurement quality.

By selecting different sensor sensitivities (adjustable in the safety controller with force limits in N), robot-dependent factors have been covered. For this study, the values 140 N, 130 N, 100 N and 50 N were used.

IV. RESULTS

A. Test on Plane Transient Contact

According to ISO/TS 15066, the MACS can be calculated with the beforementioned equations. To analyze the difference between theoretic and practical considerations, exemplary measurements were executed. Therefore, the guide rail setup is mounted on the middle position of the frame and the measurement device is positioned at the end of the mechanical stop. For the exact speed setting, a linear robot movement is used. At first, the contact situation is theoretically investigated. Secondly, those values are compared to the actual measurement results. The following information serves as input values:

Open Science Index, Mechanical and Mechatronics Engineering Vol:15, No:9, 2021 publications.waset.org/10012307.pdf

$$E = 0{,}49\,J = 0{,}49\,\frac{kg\,m^2}{s^2} \quad (1)$$

$$m_H = 0{,}6\,kg;\; M = 58\,kg;\; m_L = 6{,}041\,kg;\; d = 0{,}02m \quad (2)$$

$$F_{max} = 280\,N;\; k = 75.000\,\frac{N}{m};\, p_{\,max} = 2.800.000\,\frac{N}{m^2} \quad (3)$$

Based on this information, the MACS of the transient plane contact case is calculated using either energy, maximum permissible force, or maximum permissible pressure as a dominant criterion:

$$m_R = \frac{M}{2} + m_L = \frac{58\,kg}{2} + 6{,}041\,kg = 35{,}041\,kg \quad (4)$$

$$\mu = \left(\frac{1}{m_H} + \frac{1}{m_R}\right)^{-1} = \left(\frac{1}{0{,}6\,kg} + \frac{1}{35{,}041\,kg}\right)^{-1} = 0{,}61045\,kg \quad (5)$$

Energy-based calculations:

$$E = \frac{1}{2}\mu v_{rel}{}^2;\; v_{rel,E} = \sqrt{\frac{2E}{\mu}} = \sqrt{\frac{2*0{,}49\,\frac{kg*m^2}{s^2}}{0{,}61045\,kg}} = 1{,}267\,\frac{m}{s} \quad (6)$$

Force-based calculations:

$$v_F = \frac{F_{max}}{\sqrt{\mu k}} = \frac{280N}{\sqrt{0{,}61045\,kg*75.000\,\frac{N}{m}}} = 1{,}3085\,\frac{m}{s} \quad (7)$$

Pressure-based calculations:

$$A_{Pl} = \frac{\pi}{4}*d^2 = \frac{\pi}{4}*0{,}02\,m^2 = 3{,}142*10^{-4}\,m^2 \quad (8)$$

$$v_{P,Pl} = \frac{p_{max}*A_{Pl}}{\sqrt{\mu k}} = \frac{2.800.000\frac{N}{m^2}*3{,}1416*10^{-4}m^2}{\sqrt{0{,}61045kg*75.000\,\frac{N}{m}}} = 4{,}111\,\frac{m}{s} \quad (9)$$

Depending on the used reference basis, different speed values are calculated. Overall, the MACS exceed the maximum linear speed of the cobot of 1 m/s. While the energy- and force-based calculations lead to nearly similar results of about 1.3 m/s, the pressure-based result is nearly three times higher. Consequently, the forces and energies are the limiting factors, while pressure could be enormously increased.

The practical results deliver a much slower MACS of 645 mm/s to 647 mm/s. This deviation can be traced back to the experiment design regarding the weight of the measurement setup and friction effects of the guide rail, and the used values for the calculation. Due to the mass deviation between actual hand mass and measurement setup, the recoiling mass is much higher, which distorts the result.

For calculation, a robot mass of 58 kg was assumed, which included the whole robot, while ISO/TS 15066 describes the mass of moving robot elements. Furthermore, it is interesting to see that the sensor sensitivity does not affect the results. Due to the high contact energies, the robot stops immediately at the collision moment. In contrast to the quasi-static measurements, where the device is mounted firmly on the frame, the rail moves after the collision in the transient case. Therefore, the sensitivity takes no effect. For this experiment, measurements with a 50 N force limit setting were not possible, since the torque sensors were triggered by the robot's acceleration due to the high sensitivity, leading to a secure stop of the robot.

B. Test on Edge Transient Contact

Calculations based on maximum permissible force and energy yield the same result as specified in Subsection *A*. Therefore, only the calculations based on allowable pressures lead to different results since the size of the collision surface is significantly smaller in this case. The collision area can be simplified assumed as a rectangle.

$$A_{Ed} = 0{,}002m * 0{,}010m = 2*10^{-5}\,m^2 \quad (10)$$

$$v_{P,Ed} = \frac{p_{max}*A_{Ed}}{\sqrt{\mu k}} = \frac{2.800.000\frac{N}{m^2}*2*10^{-5}m^2}{\sqrt{0{,}61045kg*75.000\,\frac{N}{m}}} = 0{,}266\,\frac{m}{s} \quad (11)$$

Due to the small collision surface, pressure is the dominant criterion. For the whole sensor sensitivity area, an equal MACS of 80 mm/s has been identified. According to the theoretical calculations, the force is the restrictive factor, while the pressure could be highly increased. The practical measurements, however, show the opposite. Figure 4 illustrates the occurring forces and pressures at 80 mm/s (dotted) and 90 mm/s (full) operating speed relative to the threshold values. Forces are strongly undercutting the allowed values for both velocities. On the other side, pressures are very close to the threshold at a speed of 80 mm/s but exceed those limits at 90 mm/s. Irregularities in the pressure results can be traced back to the inaccuracy of the pressure-sensitive foils. Therefore, the slightly exceeding pressure value at 130 N can be considered as within the tolerance.

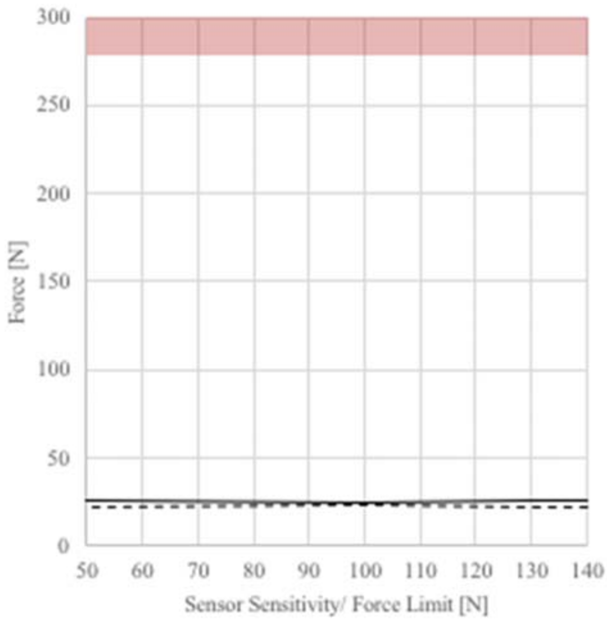

Fig. 4 Occurring Forces for Transient Edge Case at 80 mm/s (dotted) and 90 mm/s (full) operating speeds

Open Science Index, Mechanical and Mechatronics Engineering Vol:15, No:9, 2021 publications.waset.org/10012307.pdf

Open Science Index, Mechanical and Mechatronics Engineering Vol:15, No:9, 2021 publications.waset.org/10012307.pdf

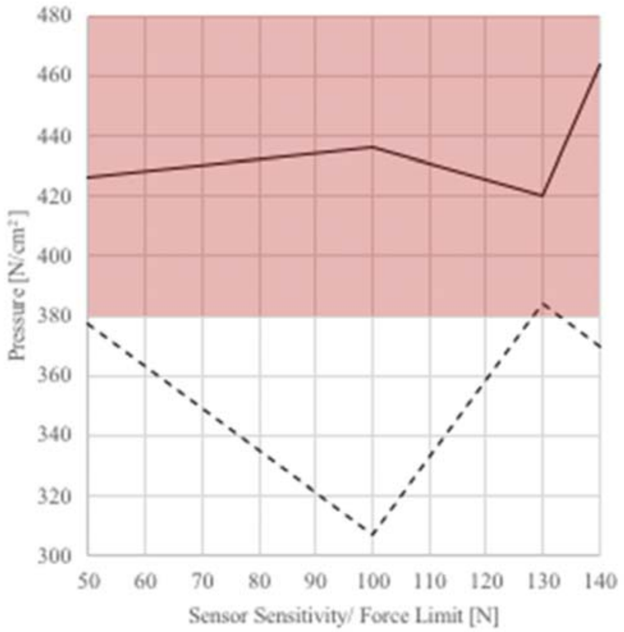

Fig. 5 Occurring Pressures for Transient Edge Case for 80 mm/s (dotted) and 90 mm/s (full)

Figure 6 shows an exemplary pressure distribution within the allowed specifications.

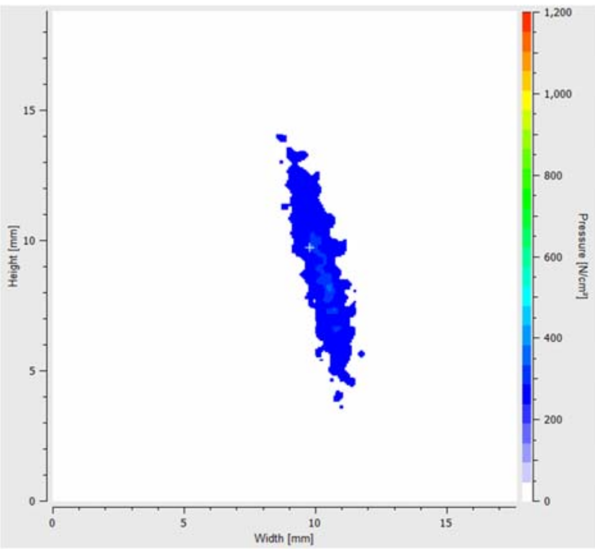

Fig. 6 Exemplary Pressure Distribution for Transient Edge Contact

V. Conclusions

In this paper the influence of the contact surface in transient contact cases have been analyzed by comparing measurements with a 20 mm diameter plane and an edge case. As body region, the back of the hand ND was assumed within the risk assessment, that could collide during a robot movement from the machine's door to a material deposit position. For theoretical backup, the equations defined in ISO/TS 15066 were used to calculate the maximum allowed speeds. It has been demonstrated that the calculated maximum velocity highly deviates depending on the utilized metric. Comparisons to the actual measured results show high differences of approximately 0.62 m/s to 3.47 m/s for the plane contact and 0.19 m/s to 1.23 m/s for the edge contact, depending on the reference basis. Especially the pressure distribution estimation seems to lack precision. Measurement deviations can be traced back to inaccuracies of the setup and the measurement procedure, especially the pressure-sensitive foils.

Since the robot safely stops immediately, the sensor sensitivity minimally influences the results. Measurements with a force limit of 50 N showed difficulties to perform due to self-triggering of the robot sensors at high velocities.

This research is limited to the selected robot model and cannot be transferred to other collaborative robots. In the future, similar tests with other models can help to build up a database of the maximum allowed collaborative speeds under consideration of different influencing factors. On the safety engineering side, such a tool would facilitate the risk assessment effort and reduce certification time and cost on the economic side. The investment reliability can be increased due to the exact determination of allowed robot velocities and, therefore, cycle times. For the robot planner and end-user, such a database supports performance transparency of different robot products and the cycle time-based selection of the most profitable robot. Lastly, robot manufacturers can follow up on these data to improve the utilized sensor technology's performance.

Future research could focus on the influence of double gripper utilization, a conversion factor to counterbalance the mass deviation between theoretical hand mass and the measurement setup as well as protective effects of different damping materials.

Acknowledgment

This project has received funding from the European Union's Horizon 2020 research and innovation program under grant agreement No 779966. We thank Dr.-Ing. Roland Behrens from the Fraunhofer Institute (IFF) for providing the technical drawings of the measurement setup and for supervising the project.

References

[1] P. Chemweno, L. Pintelon, and W. Decre, "Orienting safety assurance with outcomes of hazard analysis and risk assessment: A review of the ISO 15066 standard for collaborative robot systems," Safety Science, vol. 129, 2020, doi: 10.1016/j.ssci.2020.104832.

[2] P. A. Lasota, T. Fong, and J. A. Shah, "A Survey of Methods for Safe Human-Robot Interaction," Foundations and Trends, vol. 5, no. 4, pp. 261–349, 2014, doi: 10.1561/9781680832792.

[3] J. Marvel and R. Bostelman, "A Cross-domain Survey of Metrics for Modelling and Evaluating Collisions," International Journal of Advanced Robotic Systems, vol. 11, 2014, doi: 10.5772/58846.

[4] S. Robla-Gómez, V. M. Becerra, J. R. Llata, E. González-Sarabia, C. Torre-Ferrero, and J. Pérez-Oria, "Working Together: A Review on Safe Human-Robot Collaboration in Industrial Environments," IEEE Access, vol. 5, pp. 26754–26773, 2017, doi: 10.1109/ACCESS.2017.2773127.

[5] V. Villani, F. Pini, F. Leali, and C. Secchi, "Survey on human–robot collaboration in industrial settings: Safety, intuitive interfaces and applications," Mechatronics, vol. 55, pp. 248–266, 2018, doi: 10.1016/j.mechatronics.2018.02.009.

[6] Robots and robotic devices - Collaborative robots, ISO/TS 15066:2016, International Organization for Standardization (ISO), 2016.

[7] R. Behrens and G. Pliske, "Human-Robot Collaboration: Partial Supplementary Examination (of Pain Thresholds) for Their Suitability for Inclusion in Publications of the DGUV and Standardization," Fraunhofer IFF, Otto von Guericke University Trauma Surgery Clinic, 2019.

[8] K. Eder, C. Harper, and Z. Leonards, Eds., Towards the Safety of Human-in-the-Loop Robotics: Challenges and Opportunities for Safety Assurance of Robotic Co-Workers: IEEE, 2014.

[9] P. Svarny, J. Rozlivek, L. Rustler, and M. Hoffmann, "3D Collision-Force-Map for Safe Human-Robot Collaboration (Preprint)," 2020.

[10] S. Haddadin, A. Albu-Schäffer, and G. Hirzinger, "Safe Physical Human-Robot Interaction: Measurements, Analysis and New Insights," Robotics Research, pp. 395–407, 2011, doi: 10.1007/978-3-642-14743-2_33.

[11] B. Vemula, B. Matthias, and A. Ahmad, "A design metric for safety assessment of industrial robot design suitable for power□ and force□limited collaborative operation," International Journal of Intelligent Robotics and Applications, vol. 2, pp. 226–234, 2018, doi: 10.1007/s41315-018-0055-9.

[12] R. Weitschat, "Industrial Human-Robot Collaboration: Maximizing Performance While Maintaining Safety," Dissertation, Fakultät für Maschinenbau und Schiffstechnik, Universität Rostock, 2019.

[13] S. Haddadin, A. De Luca, and A. Albu-Schäffer, "Robot Collisions: A Survey on Detection, Isolation, and Identification," IEEE Transactions on Robotics, vol. 33, no. 6, pp. 1292–1312, 2017, doi: 10.1109/TRO.2017.2723903.

[14] M. Ganglbauer, M. Ikeda, M. Plasch, and A. Pichler, "Human in the loop online estimation of robotic speed limits for safe human robot collaboration," 30th International Conference on Flexible Automation and Intelligent Manufacturing (FAIM2021), Procedia Manufacturing 51, pp. 88–94, 2020, doi: 10.1016/j.promfg.2020.10.014.

[15] N. Kovincic et al., "A model-based strategy for safety assessment of a robot arm interacting with humans," Proceedings in Applied Mathematics & Mechanics, 2019, doi: 10.1002/pamm.201900247.

[16] H. Shin, S. Kim, K. Seo, and S. Rhim, Eds., A Real-Time Human-Robot Collision Safety Evaluation Method for Collaborative Robot: IEEE, 2019.

[17] S.-H. Yen, P.-C. Tang, Y.C. Lin, and C.-Y. Lin, "Development of a Virtual Force Sensor for a Low-Cost Collaborative Robot and Applications to Safety Control," Sensors, vol. 19, no. 11, 2019, doi: 10.3390/s19112603.

[18] C. Schneider, T. Suchanek, M. Klos, and M. Hutter-Mironovová, COVR Project RACOS: Risk Assessment Metamodel for Cobot Operating Speed Determination. (Online). Available: https://covrfilestorage.blob.core.windows.net/documents/casestories%5CRACOS%20Milestone%201.pdf (accessed: Aug. 14 2021).

[19] DGUV, Collaborative robot systems: Design of systems with "Power and Force Limiting" function. (Online) Available: https://www.dguv.de/medien/fb-holzundmetall/publikationen-dokumente/infoblaetter/infobl_englisch/080_collaborativerobotsystems.pdf (accessed: Apr. 12 2019).

Open Science Index, Mechanical and Mechatronics Engineering Vol:15, No:9, 2021 publications.waset.org/10012307.pdf